

A High Power High Voltage Step-Up Dc-Dc Converter for Grid Connected Renewable Energy Sources**N.Vivek Babu, E.Nagaraju, D.Suman, K.Raju**¹B.Tech scholars, Dept of EEE, SVS Institute of Technology, Hanamkonda, Warangal, T.S, India**Mr.D.Kumaraswamy (Ph.D)**² Associate Professor, Dept of EEE, SVS Institute of Technology, Hanamkonda, Warangal, T.S, India**Abstract**

With the rapid development of large-scale renewable energy sources and HVDC grid, it is a promising option to connect the renewable energy sources to the HVDC grid with a pure dc system, in which high-power high-voltage step-up dc-dc converters are the key equipment to transmit the electrical energy. This paper proposes a resonant converter which is suitable for grid-connected renewable energy sources. The converter can achieve high voltage gain using an LC parallel resonant tank. It is characterized by zero-voltage-switching (ZVS) turn-on and nearly ZVS turn-off of main switches as well as zero-current-switching turn-off of rectifier diodes; moreover, the equivalent voltage stress of the semiconductor devices is lower than other resonant step-up converters. The operation principle of the converter and its resonant parameter selection is presented in this paper. The operation principle of the proposed converter has been successfully verified by simulation and experimental results.

Keywords: Renewable Energy, Resonant Converter, Soft Switching, Voltage Step-Up, Voltage Stress.**1. Introduction**

THE dc grid, with the advantages such as reactive power, harmonics, and so on [1], seems to be a promising solution of power collection system for the growing demand in the offshore wind power development. The offshore wind turbines may be directly connected into a dc grid to deliver dc power to medium or high-dc voltage network [2]. To realize the dc connection and power delivery, a high-efficient dc/dc converter is required. Normally, the voltage level of the dc network would be dozens of kilovolts which is much higher than the input voltage of the dc/dc converter [2]. Hence, a medium frequency transformer(MFT) operated at hundreds of hertz to several kilohertz would be installed in the dc/dc converter, which not only ensures that the input voltage can be boosted to a desired high output voltage, but also achieves the galvanic isolation between source and grid. Besides, owing to the high-voltage level in the dc network, the usage of the diode bridges in the dc/dc converters could be advantageous. A number of converters are presented in [3]–[23]. The two level and three-level configurations are mainly considered here, since both of the two configurations have been widely used in the wind energy system [24]. Fig. 1 shows several possible/dc converters for the dc-grid wind turbine, including the basinful-bridge (FB) two-level converter, the basic half-bridge) three-level converter, the basic FB three-level converter, and the FB three-level converter based on sub modules (SMs).The four converter configurations for an example of a 2.5-MW wind turbine system are considered in Table I. The system parameters are listed in the Appendix. The rated input voltage of the converters is 5.4 kV, and the 1700 V/600 A insulated gate bipolar transistor (IGBT) (FZ600R17KE3) with the nominal device voltage V_{com} at 100 FIT as 900 V is applied for the different converter configurations [25]. Although the required switch number for the FB two-level converter are not so many among the four configurations,

the switches in the two-level configurations have to take the full dc-bus voltage. The voltage change rate dv/dt is high; therefore, it may cause large electromagnetic interference (EMI) [3]–[6]. As the three-level converters with the advantages in the aspects of power quality, semiconductor electrical and thermal stresses, and EMI for high-power applications [7]–[17], the switches in the basic HB three-level converter, FB three-level converter, and the SMs-based FB three-level converter only take half of the dc bus voltage, which effectively reduces dv/dt in comparison with the FB two-level converter. For the N-level configuration, a total number of $8(N-1)$ switches are needed for the SMs-based FB converter, which is much more than $2(N-1)$ and $4(N-1)$ switches required in the basic HB and FB converters, respectively [7], [18]. Besides, the corresponding numbers of voltage sensors are normally required for the SMs, and the voltage balancing control would be complicated for the SMS-based FB converter [19]. The basic full-bridge three-level (FBTL) converter, with the advantage of the reduced voltage stress of the switches, reduced filter size, and improved dynamic response, is becoming highly suitable for medium-voltage and high-power conversion [7]. Although both the basic FBTL and the SMs-based FBTL configurations can create five-level output voltage to minimize voltage steps and reduce dv/dt in comparison with the basic HBTL configuration, particularly in the medium-voltage and high-power applications [18], [26], [27], the basic FBTL converter has a simpler circuit structure and less number of switch devices than the SMs-based FBTL configuration, which leads to a small footprint and high reliability for the basic FBTL converter. The FB converter has been evaluated to be a suitable choice for wind farm application from an energy efficiency point of view [28]. Hence, the isolated FBTL dc/dc converter is to be studied for high-power wind turbine systems in this paper. Some work about the isolated FBTL converter control has been reported, such as the chopping phase-shift (CPS) control and double phase-shift (DPS) control presented in [8] and [9], respectively, but they have a high-voltage change rate dv/dt , and

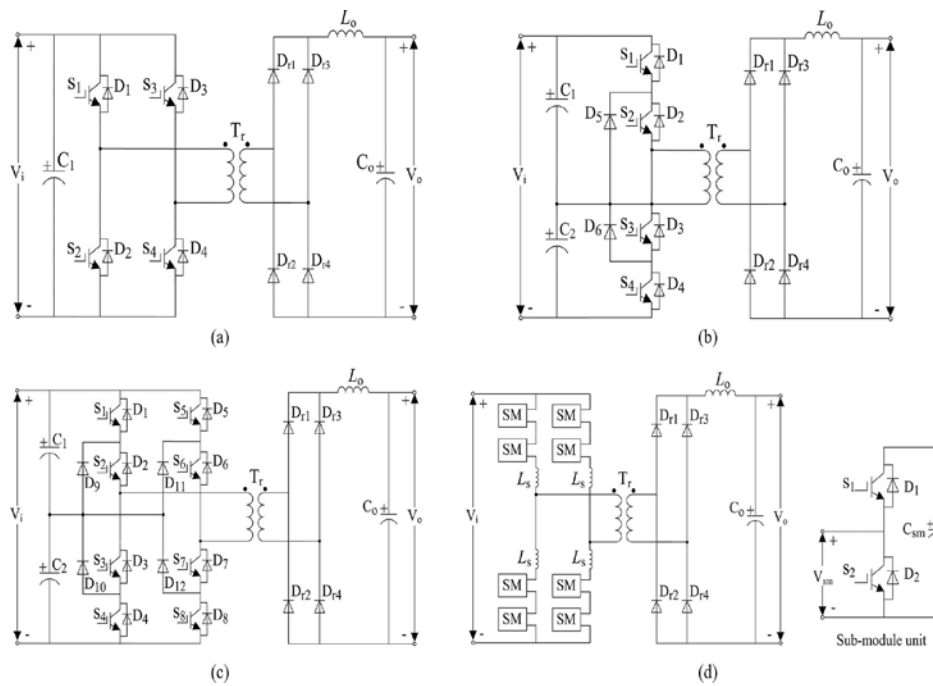


Figure 1: Basic FB two-level converter. (b) Basic HB three-level converter. (c) Basic FB three-level converter. (d) SMs based-FB three-level converter.

TABLE I
POSSIBLE DC/DC CONVERTER OPTIONS

| Converter topology | Valve number | Switch number in each valve | Valve voltage | Produced voltage level | Voltage balance control complexity | Voltage sensor |
|-----------------------------------|--------------|-----------------------------|---------------------|------------------------|---|----------------|
| 2-level Basic FB converter | 4 | 6×1.7 kV IGBTs | DC bus voltage | 2 | No | 1 |
| 3-level Basic HB converter | 4 | 3×1.7 kV IGBTs | Half DC bus voltage | 3 | Easy | 2 |
| 3-level Basic FB converter | 8 | 3×1.7 kV IGBTs | Half DC bus voltage | 5 | Easy | 2 |
| 3-level FB converter based on SMs | 16 | 3 ×1.7 kV IGBTs | Half DC bus voltage | 5 | Calculation is proportional to the SMs number | 8 |

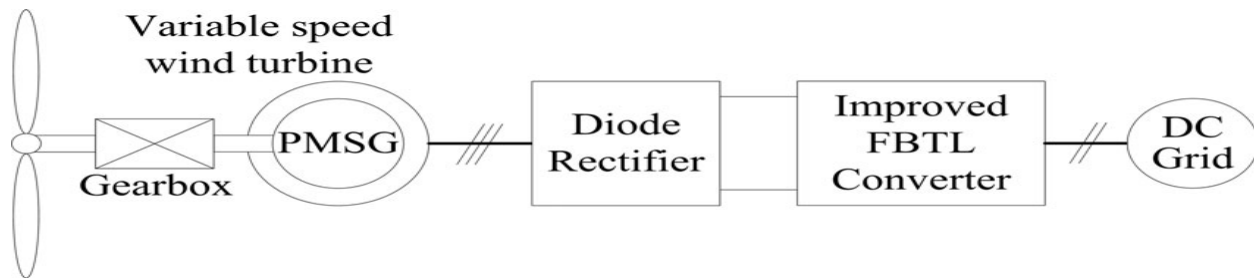


Figure 2: Block diagram of the wind turbine connected to a dc grid

Thus may not be applicable for the medium-voltage and high power systems. So far, the application of the isolated FBTLdc/dc converter for offshore wind turbines within a dc grid has not been addressed in detail in the literature. In this paper, an improved FBTL (IFBTL) dc/dc converter is presented for an offshore wind turbine based on permanent magnet synchronous generators (PMSGs) in a dc grid where the IFBTL dc/dc converter is applied to boost the DC voltage from a diode rectifier to a high voltage for the dc grid integration. This paper is organized as follows. In Section II, the IFBTLdc/dc converter and the corresponding modulation strategy are proposed. In Section III, the voltage balancing control for the IFBTL dc/dc converter is proposed. Section IV presents the control of the wind turbine system based on the IFBTL dc/converter. A 1-kW prototype is built and tested in the laboratory.

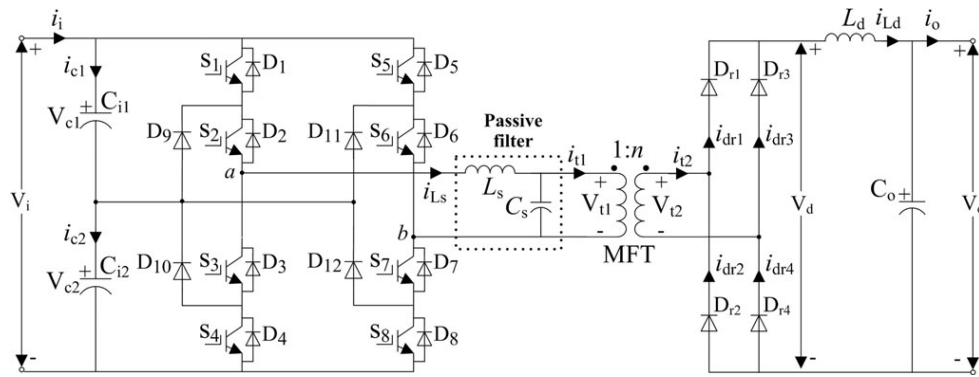


Figure 3: Block diagram of the IFBTL dc/dc converter.

And the results verify the feasibility of the proposed converter topology, modulation strategy, and voltage balancing control strategy, which is reported in Section V. Finally, the main conclusions are drawn in Section VI.

2. IFBTL DC/DC Converter

A. Converter Description

Fig. 3 shows the configuration of the IFBTL dc/dc converter, which is composed of eight switches (S1–S8), eight freewheeling diodes (D1–D8), four clamping diodes (D9–D12), an MFT, four rectifier diodes (Dr 1–Dr 4), a passive filter (L_s and C_s), an output filter inductor L_d , an output capacitor C_o , and two voltage divided capacitors (C_{i1} and C_{i2}), which are used to split the dc bus voltage V_i into two equal voltages V_{c1} and V_{c2} . Different from the FBTL dc/dc converter, a passive filter is inserted into the IFBTL dc/dc converter as shown in Fig. 3 to improve the performance of the dc/dc converter [29], which can effectively overcome the problem that the nonlinear characteristics of semiconductor devices result in distorted waveforms associated with harmonics and reduce the voltage stress of the MFT, which is very significant for the power converter in the high-power application's. Proposed Modulation Strategy The switches S1–S8 are switched complementarily in pairs with a pulse width modulation (PWM), i.e., pairs S1–S3, S4–S2, S5–S7, and S8–S6, respectively. The duty cycle for S1 is D . The way of phase shifting the PWM for other switch pairs results in the different operation modes as follows. 1) Operation Mode I: The PWM waveform for the pairs S8–S6, S5–S7, and S4–S2 lags behind that for pair S1–S3 by $(D - D_c)T_s/2$, $T_s/2$, and $(D - D_c + 1)T_s/2$ respectively as T_s is the switching cycle. The overlap time between S1–S3 and S8–S6 is $D_cT_s/2$, which is also for S4–S2 and S5–S7. D_c is defined as the overlap duty ratio. 2) Operation Mode II: The PWM waveform for pair S8–S6 leads before that for pair S1–S3 by $(D - D_c)T_s/2$, and the PWM waveform for pairs S4–S2 and S5–S7 lags behind that for the pair S1–S3 by $(1 - D + D_c)T_s/2$ and $T_s/2$, respectively, as shown in Fig. 4(b). The overlap time between S1–S3 and S8–S6, and between S4–S2 and S5–S7 is also both $D_cT_s/2$. The main difference between the two operation modes is the capacitor charge and discharge situations in each half cycle as in operation mode I, capacitor C_{i2} discharges more energy than capacitor C_{i1} in each half cycle as while capacitors C_{i1} and the C_{i2} exchange their situations in operation mode II as shown in In operation mode II, capacitor C_{i1} discharges more energy than capacitors' 2 in each half cycle. The two operation modes can be alternatively used for the adaptive voltage balancing control, which will be described in Section III. The steady-state operations of the converter under the proposed modulation strategy are explained with the assumption that $C_{i1} = C_{i2}$. Fig. 4 shows the simulation waveforms of the IFBTL dc/dc converter in one cycle T_s under operation modes I and II, respectively. The

system parameters are given in , voltages V_{ab} , V_{t1} , V_{t2} and currents i_{Ls} , i_{t1} , i_{t2} are all periodic waveforms with period T_s . Currents i_{c1} , i_{c2} , and i_{Ld} with the period $T_s/2$. Owing to the passive filter in the IFBTLdc/dc converter, the performance of voltages V_{t1} , V_{t2} and currents i_{t1} , i_{t2} associated with the MFT is effectively improved, which is significant for the IFBTL dc/dc converter in the applications of the medium-voltage and high-power system. From it is easy to see that the charge and discharge situations (i_{c1} and i_{c2}) of capacitors C_{i1} and C_{i2} are the main difference between the operation modes I and II, which would affect the capacitor voltages V_{c1} and V_{c2} . The other performances of the converter are nearly the same.

3. Proposed Voltage Balancing Control Strategy

A voltage balancing control strategy is proposed for the IFBTL dc/dc converter in this section, which can be realized by alternating the operation modes I and II.

A. In Operation Mode I

Both the capacitor currents i_{c1} and i_{c2} are with the period of $T_s/2$. In the first half cycle, the charge or discharge situations for capacitors C_{i1} and C_{i2} in stages A, C, and E are the same. In stage B, current i_{c2} is more than i_{c1} , while i_{c2} is far less than i_{c1} in stage D as shown in Fig. 4(a). Owing to that, the periods of stages B and D are $(D - D_c) T_s/2$. Suppose $V_{c1} = V_{c2} = V_i/2$; C_{i2} would provide more energy to the load than C_{i1} in the first half cycle under the operation mode I. The situation in the second half cycle is similar to that in the first half cycle.

Consequently, voltage V_{c1} would be increased and voltage V_{c2} would be reduced in operation mode I which would result in the trend that voltage V_{c1} would be more than V_{c2} in operation mode I.

B. In Operation Mode II

The same to operation mode I, the charge and discharge situations for capacitors C_{i1} and C_{i2} in stages A, C, and E are the same as in the first half cycle. The only difference is that current

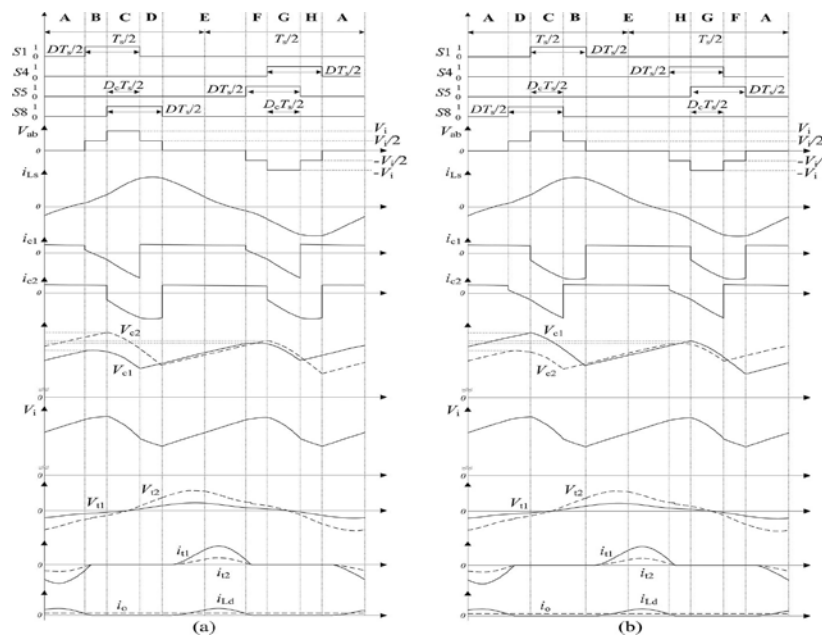


Figure 4: Key waveforms of the IFBTL dc/dc converter. (a) In operation mode I. (b) In operation mode II

ic 2 is less than ic 1 in stage D, while ic 2 is far more than ic 1 in stage B in operation mode II as shown in Fig. 4(b), which is contrary to that in operation mode I. The periods for stages B and D are both $(D - D_c) T_s / 2$. Suppose $V_{c1} = V_{c2} = V_i / 2$; C_{i1} would provide more energy to the load than C_{i2} in the first half cycle under the operation mode II. The situation in the second half cycle is similar to the first half cycle. Therefore, voltage 1 would be reduced and voltage V_{c2} would be increased in operation mode II as , which would result in the trend that voltage V_{c1} would be less than V_{c2} in operation mode II

C. Proposed Voltage Balancing Control Strategy

Based on the aforesaid analysis, V_{c1} would be more than V_{c2} in operation mode I, and V_{c1} would be less than V_{c2} in Operation mode II. Consequently, a control strategy is proposed for the capacitor voltage balancing as shown in where a comparator is used here with two input voltages V_{c1} and V_{c2} .If V_{c1} is more than V_{c2} , the operation mode in the next half cycle is selected as II. On the contrary, the operation mode I is selected in the next half cycle when V_{c1} is less than V_{c2}

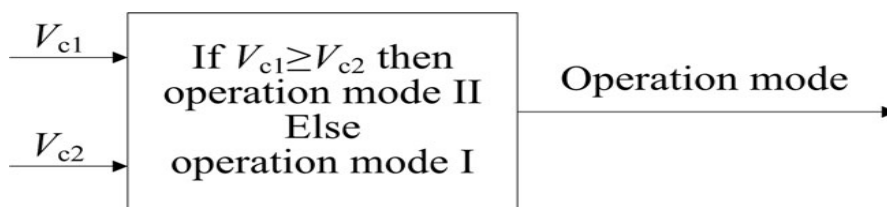


Figure 5: Block diagram of the proposed voltage balancing control for IFBTL converter.

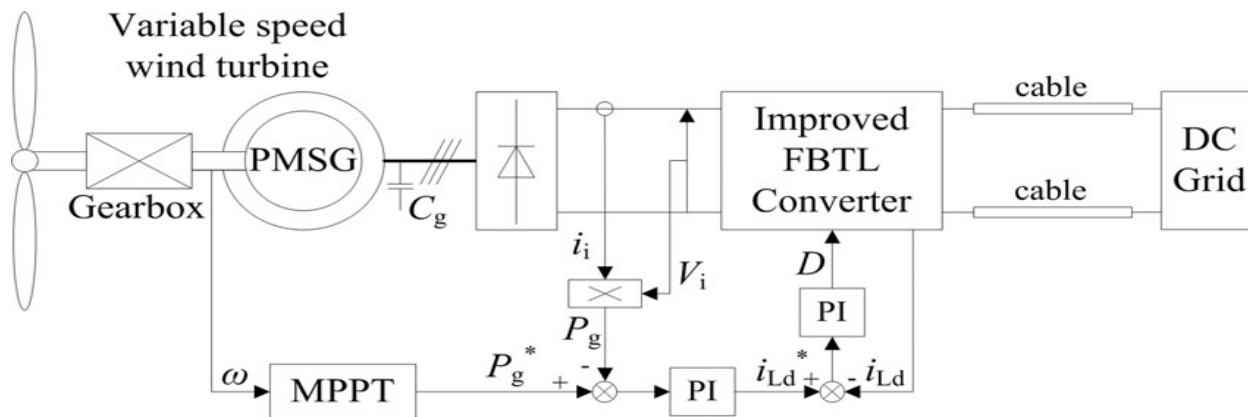


Figure 6: Block diagram of the control for the VSWT based on a PMSG and an IFBTL dc/dc converter

4. Experimental Verification

To verify the proposed function of the IFBTL dc/dc converter, a 1-kW converter prototype was built as The switching frequency is 5 kHz. The eight primary switches and diodes S1/D1–S8/D8 are the standard power MOSFET of IXTH30N25. The clamping diodes D9–D12 are STTH3006. The rectifier diodes Dr 1–Dr 4 are STTH3010. A transformer

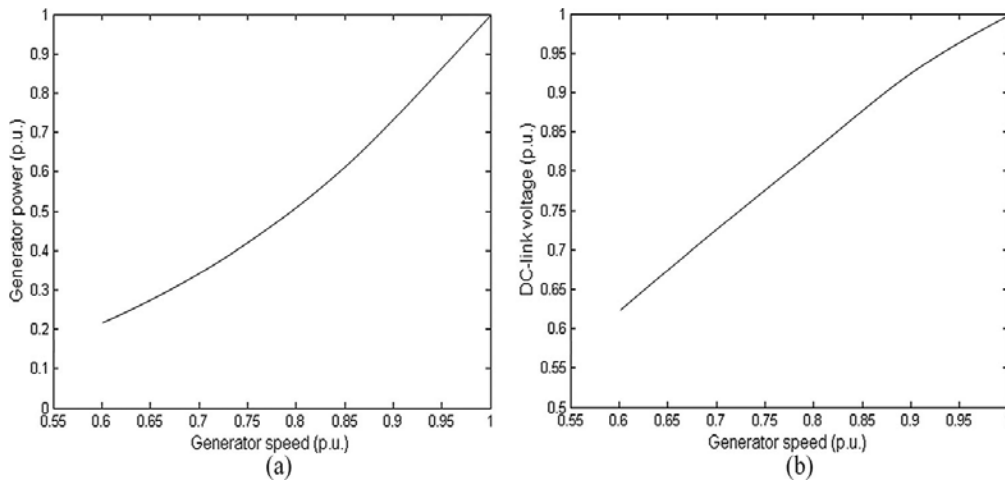


Figure 7: (a) Optimal generator power P_g under the different wind turbine speed ω . (b) Optimal dc-link voltage V_i under the different wind turbine speed ω .

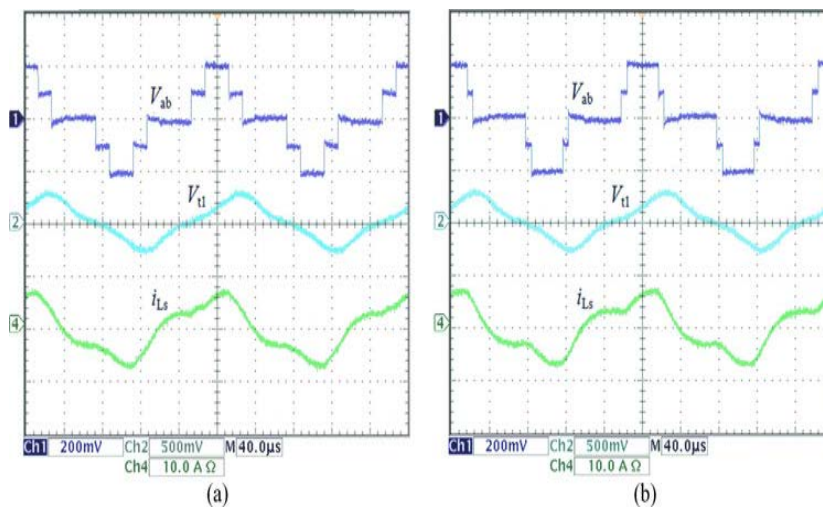


Figure 8: Measured converter waveforms including V_{ab} (100 V/div), V_{t1} (250 V/div), and i_{Ls} (10 A/div). (a) $D_c/D = 65\%$. (b) $D_c/D = 85\%$. Time base is 40 μ s/div.

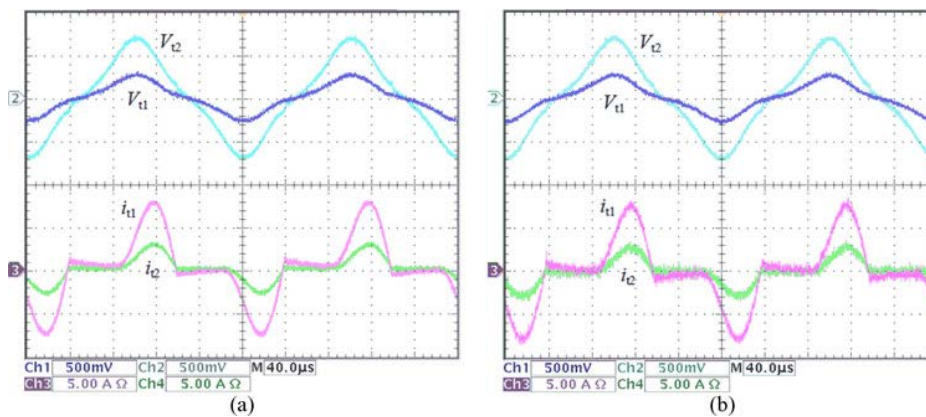


Figure 9: Measured converter waveforms including V_{t1} (250 V/div), V_{t2} (250 V/div), i_{t1} (5 A/div), and i_{t2} (5 A/div). (a) $D_c/D = 65\%$. (b) $D_c/D = 85\%$. Time base is 40 μ s/div.

With a turn ratio of 1:2.6 is used. The transformer core is aPM87/70 ferrite core, and the leakage inductance is 10 μ H. The filter inductor L_s and capacitor C_s are 0.44 mH and 3 μ F, respectively. Inductor L_d is 0.8 mH and Capacitor C_o is 1mF. The input capacitors, both $C_i 1$ and $C_i 2$, are 400 V/330 μ F. The dead time is set as 1.5 μ s. A three-phase autotransformer followed by a three-phase diode rectifier is employed at the input side to produce the input voltage V_i . A dc power supply (SM300-10D) parallel with a resistor load of 50 Ω at the output side to emulate the dc grid and support the constant output voltage V_o as 250 V. An inductor with the value of 0.4 mH is inserted between the output of the converter and the dc power supply. In order to verify the feasibility of the IFBTL dc/dc converter for wind turbines, the two curves of the optimal power versus

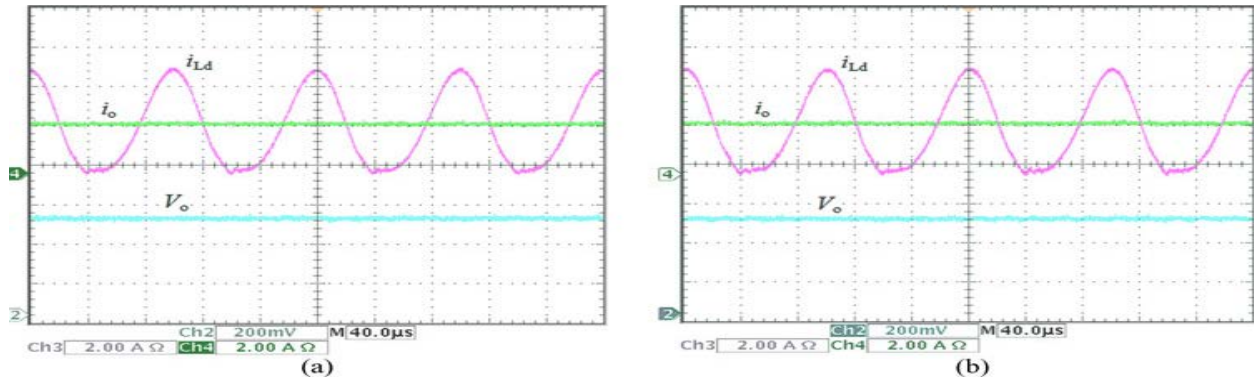


Figure 10: Measured converter waveforms including V_o (100 V/div), i_{Ld} (2 A/div), and i_o (2 A/div). (a) $D_c / D = 65\%$. (b) $D_c / D = 85\%$. Time base is 40 μ s/div.

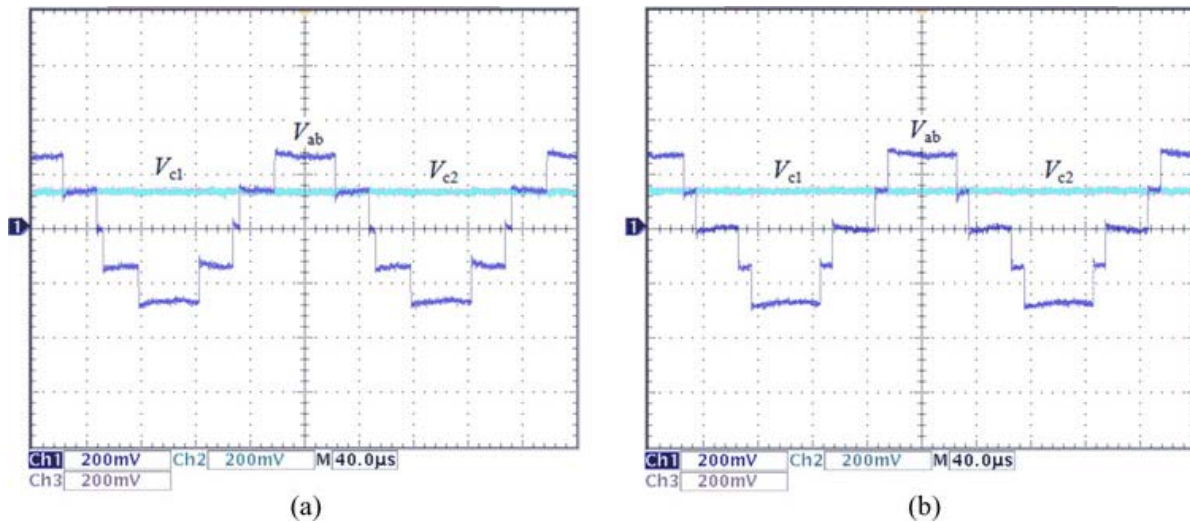


Figure 11 : Measured converter waveforms including capacitor $C_i 1$ voltage $V_c 1$ (50V/div), capacitor $C_i 2$ voltage $V_c 2$ (50V/div), and inductor current i_o (0.5 A/div) under $D_c / D = 65\%$. (a) Inductor current i_o step up. (b) Inductor current i_o step down. Time base is 1 ms/div

5. Conclusion

This paper has presented the control of the IFBTL dc/converter for the wind turbine system to facilitate the integration of wind turbines into a dc grid. The corresponding modulation strategy, including operation modes I and II, is proposed for the IFBTL dc/dc converter. The proposed two operation modes are discussed in detail. A voltage balancing control

strategy is proposed for the IFBTL dc/dc converter, where the alternation of the proposed two operation modes can keep the capacitor voltage balanced. With the passive filter and the modulation strategy, the voltage stress of the transformer in the IFBTL dc/converter can be effectively reduced, which is very significant in the medium-voltage and high-power application. The control of the wind turbine system based on the IFBTL dc/dc converter is presented as well. A laboratory prototype of 1-kW IFBTL dc/converter has been tested, and the results show good agreement with the theoretical analysis in this paper.

6. References

- [1] C. Meyer, M. Hoing, A. Peterson, and R. W. De Doncker, "Control and design of dc grids for offshore wind farms," *IEEE Trans. Ind. Appl.*, vol. 43, no. 6, pp. 1475–1482, Nov./Dec. 2007.
- [2] J. Robinson, D. Jovcic, and G. Joós, "Analysis and design of an offshore wind farm using a MV DC grid," *IEEE Trans. Power Delivery*, vol. 25, no. 4, pp. 2164–2173, Oct. 2010.
- [3] F. Blaabjerg, Z. Chen, and B. S. Kjaer, "Power electronics as efficient interface in dispersed power generation systems," *IEEE Trans. Power Electron.*, vol. 19, no. 5, pp. 1184–1194, Sep. 2004.
- [4] F. Blaabjerg, F. Iov, Z. Chen, and K. Ma, "Power electronics and controls for wind turbine systems," in *Proc. IEEE Int. Energy Conf. Exhib.*, Dec. 2010, pp. 333–344.
- [5] N. Mohan, T. M. Undeland, and W. P. Robbins, *Power Electronics: Converters, Applications, and Design*, 3rd ed. New York: Wiley, 2003.
- [6] N. Y. Dai, M. C. Wong, and Y. D. Han, "Application of a three-level NPC inverter as a three-phase four-wire power quality compensator by generalized 3DSVM," *IEEE Trans. Power Electron.*, vol. 21, no. 2, pp. 440–449, Mar. 2006.
- [7] X. Ruan, B. Li, Q. Chen, S. C. Tan, and C. K. Tse, "Fundamental considerations of three-level dc-dc converters: Topologies, analyses, and control," *IEEE Trans. Circuits Syst. I, Reg. Papers*, vol. 55, no. 11, pp. 3733–3743, Dec. 2008.
- [8] Z. Zhang and X. Ruan, "ZVS PWM full-bridge three-level converter," in *Proc. 4th Int. Power Electron. Motion Control Conf.*, 2004, pp. 1085–1090.
- [9] Z. Zhang and X. Ruan, "A novel double phase-shift control scheme for full-bridge three-level converter," in *Proc. 20th Annu. IEEE Appl. Power Electron. Conf. Expos.*, Mar. 2005, pp. 1240–1245.
- [10] P. J. Grbovic, "High-voltage auxiliary power supply using series connected MOSFETs and floating self-driving technique," *IEEE Trans. Ind. Electron.*, vol. 56, no. 5, pp. 1446–1455, May 2009.
- [11] P. J. Grbović, P. Delarue, P. Le Moigne, and P. Bartholomeus, "A bidirectional three-level dc-dc converter for the ultracapacitor applications," *IEEE Trans. Ind. Electron.*, vol. 57, no. 10, pp. 3415–3430, Oct.
- [12] P. M. Barbosa, F. Canales, J. M. Burdío, and F. C. Lee, "A three-level converter and its application to power factor correction," *IEEE Trans. Power Electron.*, vol. 20, no. 6, pp. 1319–1327, Nov. 2005.
- [13] J. R. Pinheiro and I. Barbi, "The three-level ZVS-PWM dc-to-dc converter," *IEEE Trans. Power Electron.*, vol. 8, no. 4, pp. 486–492, Oct. 1993.
- [14] S. Inoue and H. Akagi, "A bidirectional isolated dc-dc converter as a core circuit of the next-generation medium-voltage power conversion system," *IEEE Trans. Power Electron.*, vol. 22, no. 2, pp. 535–542, Mar. 2007.

- [15] M. Malinowski, K. Gopakumar, J. Rodriguez, and M. A. P´erez, “A survey on cascaded multilevel inverters,” *IEEE Trans. Ind. Electron.*, vol. 57, no. 7, pp. 2197–2206, Jul. 2010.
- [16] S. Kouro, M. Malinowski, K. Gopakumar, J. Pou, L. G. Franquelo, B. Wu, J. Rodriguez, M. A. P´ere, and J. I. Leon, “Recent advances and industrial applications of multilevel converters,” *IEEE Trans. Ind. Electron.*, vol. 57, no. 8, pp. 2553–2580, Aug. 2010.
- [17] J. Rodriguez, S. Bernet, B. Wu, J. O. Pontt, and S. Kouro, “Multilevel voltage-source-converter topologies for industrial medium-voltage drives,” *IEEE Trans. Ind. Electron.*, vol. 54, no. 6, pp. 2930–2945, Dec. 2007.
- [18] S. Kenzelmann, A. Rufer, M. Vasiladiotis, D. Dujic, F. Canales, and Y. R. de Novaes, “A versatile dc–dc converter for energy collection and distribution using the modular multilevel converter,” in *Proc. 14th Eur. Conf. Power Electron. Appl.*, Aug./Sep. 2011, pp. 1–10.
- [19] M. Saeedifard and R. Iravani, “Dynamic performance of a modular multilevel back-to-back HVDC system,” *IEEE Trans. Power Delivery*, vol. 25, no. 4, pp. 2903–2912, Oct. 2010.
- [20] M. A. Parker, N. Chong, and R. Li, “Fault-Tolerant control for a modular generator-converter scheme for direct-drive wind turbines,” *IEEE Trans. Ind. Electron.*, vol. 58, no. 1, pp. 305–315, Jan. 2011.
- [21] R. Mel´icio, V. M. F. Mendes, and J. P. S. Catalˆao, “Comparative study of power converter topologies and control strategies for the harmonic performance of variable-speed wind turbine generator systems,” *Energy*, vol. 36, no. 1, pp. 520–529, Jan. 2011.